

Article

Research on the Preparation Process of SBS-Modified Asphalt Using Early Shearing Instead of High-Speed Shearing of Modifier

Yanlei Wang¹, Hongyu Yi^{2,*}, Yong Cui¹, Shijiang Li¹, Shengxiong Zhou³ and Chuanqi Yan³

¹ Shandong Road and Bridge Group Co., Ltd., Jinan 250014, China; 13551269757@163.com (Y.W.); 19180964367@163.com (Y.C.); shijiangli2023@163.com (S.L.)

² China Railway Development Investment Group Co., Ltd., Kunming 650200, China

³ Highway Engineering Key Laboratory of Sichuan Province, Civil Engineering School, Southwest Jiaotong University, Chengdu 610031, China; zhoushengxiong2022@163.com (S.Z.); ycq@swjtu.edu.cn (C.Y.)

* Correspondence: yihongyu@my.swjtu.edu.cn; Tel.: +86-191-8096-4367

Abstract: To investigate the effect of pre-shredding as a replacement for high-speed shearing in the preparation process of SBS-modified asphalt, the particle size and mixing time of pre-shredded SBS modifier were studied. Laser confocal microscopy was used to observe the morphological changes and dispersion state of the SBS modifier during the mixing process, and process parameters were determined through rheological performance tests. FTIR tests were conducted on the original asphalt and PAV-aged modified asphalt to assess the impact of the pre-shredding process on the chemical composition and aging resistance of the modified asphalt. The specific conclusions were as follows. During the preparation process of the SBS modifier using low-speed mixing, the morphological changes of the SBS modifier can be summarized as follows: It cycles through edge networking, mesh fiberization, and filamentous granulation, and eventually presents a granular atomization form after multiple cycles. It is recommended that the mixing time be maintained between 30 and 60 min, which results in the microstructure of the modified asphalt consisting of filamentous and point-like combinations. This asphalt exhibited excellent performance in high-temperature rut resistance, fatigue resistance, and low-temperature crack resistance. When the mixing time was too long, the SBS modifier formed small granules in an atomized state, which weakened the strength of the mesh structure and led to a decrease in overall performance. It is recommended that the SBS be shredded into particles sized between 18 and 30 mesh or 30 and 100 mesh. SBS-modified asphalt with SBS particles sized between 18 and 30 mesh exhibited greater hardness in the mesh structure, resulting in better high-temperature rut resistance. SBS-modified asphalt with SBS particles sized between 30 and 100 mesh had better extensibility in the mesh structure, leading to superior performance in medium-temperature fatigue resistance and low-temperature crack resistance. Compared to the conventional process, the pre-shredding process for preparing SBS-modified asphalt improved aging resistance by 10% to 13%. Additionally, SBS-modified asphalt prepared using the pre-shredding process saved 1 to 3 h of processing time compared to the traditional preparation method, reducing energy consumption. Furthermore, the asphalt produced through the new process exhibited better performance, reducing road wear and saving maintenance costs.

Keywords: SBS-modified asphalt preparation process; pre-cutting; microstructure; rheological properties



Citation: Wang, Y.; Yi, H.; Cui, Y.; Li, S.; Zhou, S.; Yan, C. Research on the Preparation Process of SBS-Modified Asphalt Using Early Shearing Instead of High-Speed Shearing of Modifier. *Appl. Sci.* **2023**, *13*, 10335. <https://doi.org/10.3390/app131810335>

Academic Editor: Luis Picado Santos

Received: 11 August 2023

Revised: 3 September 2023

Accepted: 6 September 2023

Published: 15 September 2023



Copyright: © 2023 by the authors. Licensee MDPI, Basel, Switzerland. This article is an open access article distributed under the terms and conditions of the Creative Commons Attribution (CC BY) license (<https://creativecommons.org/licenses/by/4.0/>).

1. Introduction

In recent years, SBS-modified asphalt has attracted significant attention as an important road material [1,2]. Its unique properties enable roads to maintain excellent elasticity and durability under different climate and load conditions [3,4]. However, the preparation process of SBS-modified asphalt plays a crucial role in achieving these advantages [5–7]. In

previous studies, scholars have extensively explored various preparation factors to ensure optimal performance, as shown in Table 1 [8–12].

Table 1. Recommended preparation methods from the relevant literature [13].

Author	Evaluation Indicators	Shear Rate	Shear Temp.	Shear Time	Development Time
Yan Wang	Softening point, penetration, ductility	—	180 °C	1 h	3 h
Yanming Hou	Softening point, penetration, ductility	3000 r/min	175 °C	1 h	1 h
Fuqiang Dong	Softening point, penetration, ductility	3000 r/min	200 °C	1 h	—
Yufeng Cong	Softening point, penetration, ductility	8000 r/min	180 °C	2 h	1 h
Mojtaba Mortezaei	Softening point, ductility	1500 r/min	—	—	—

Optimization of process parameters is one of the key factors in enhancing the performance of SBS-modified asphalt [14,15]. Variations in SBS dosage, addition time, and mixing speed directly impact the performance of SBS-modified asphalt [16–19]. By optimizing the SBS dosage, it is possible to increase the material's elastic modulus without affecting the fundamental properties of the asphalt, thus improving the road's resistance to deformation and extending its lifespan [20]. Precise adjustment of the modifier addition time and mixing speed parameters ensures the even dispersion of SBS in the asphalt, thereby enhancing the asphalt's crack resistance, elasticity, and deformation capabilities [21].

Furthermore, control over the mixing temperature is also crucial for the success of the modification process [22,23]. During preparation, an appropriate mixing temperature can facilitate a thorough blending of SBS and asphalt, ensuring the effectiveness of their interaction [24]. Too low a temperature can result in incomplete dispersion of the SBS polymer in the asphalt, impacting material performance [25]. Conversely, excessively high temperatures can lead to polymer degradation, thereby reducing the modification's effectiveness [26]. Therefore, researchers must accurately control the mixing temperature during the process to ensure optimal modification effects.

The optimization of polymer dispersion in the preparation process directly influences the overall performance of SBS-modified asphalt [27,28]. Therefore, polymer dispersion is a critically important consideration. By using suitable dispersing agents and mixing processes, it is possible to minimize the formation of polymer aggregates, thus enhancing the material's uniformity. Similarly, optimizing the dispersion process ensures the even distribution of SBS polymers within the asphalt matrix, significantly boosting the material's stability and performance. By selecting appropriate dispersing agents and optimizing the mixing process, it is possible to effectively reduce the formation of polymer aggregates, greatly enhancing the material's uniformity [29,30].

In conclusion, the performance advantages of SBS-modified asphalt largely depend on the optimization of its preparation process. Adjustments to process parameters, polymer dispersion, and the control of mixing temperatures all play crucial roles in ensuring the exceptional performance of the final product. In-depth research into these key factors can support the continuous optimization of SBS-modified asphalt materials, providing more durable and reliable materials for road construction.

Building upon the extensive work of previous researchers, this paper proposes the pre-shredding of the SBS modifier as a replacement for the high-speed shearing step, focusing on the pre-shredded particle size and mixing time parameters of the SBS. In order to compare the microstructural and rheological properties of pre-shredded SBS-modified asphalt with those of asphalt prepared using conventional methods and to optimize the pre-shredded particle size and mixing time parameters, laser confocal microscopy experiments

and dynamic shear rheometer (DSR) tests were conducted. Ultimately, the recommended preparation parameters are those that exhibited strong dispersion uniformity, excellent resistance to rutting at high temperatures, resistance to fatigue at intermediate temperatures, and optimal resistance to cracking at low temperatures.

2. Materials and Methods

2.1. Materials

This study employed ES70# as the base asphalt, with performance parameters as shown in Table 2. SBS-161B is produced by PetroChina Kunlun Dushanzi Petrochemical Company in China, with an average molecular weight of 200,000 g/mol and other performance parameters as shown in Table 3. A sulfur-based stabilizer was used as the stabilizer.

Table 2. Main technical indicators of E70# asphalt.

Performance	Unit	Requirement of ES70# Asphalt	Result
Penetration (25 °C, 5 s, 100 g)	0.1 mm	60–80	68
Ductility (5 cm/min)	cm	≥15	16.8
	15 °C	≥100	>100
Softening point	°C	≥46	46.2
Density (15 °C)	g/cm ³	Measured	1.030
Brookfield viscosity (135 °C)	Pa·s	-	0.65

Table 3. Performance parameters of the SBS modifiers.

Grade	Structural Type	Block Copolymer Ratio	Tensile Strength (≥MPa)	Elongation at Break (≥%)	Shore Hardness (A)	Melt Flow Rate (g/10 min)
T-161B	star	30/70	17.7	700	82	0.5

2.2. Pre-Cutting Process for SBS

The SBS modifier cutting process is illustrated in Figure 1. After undergoing shredding in a grinder, the shredded SBS was classified into three grades using a vibrating sieve: 18 to 10 mesh (1 to 2 mm), 30 to 18 mesh (0.6 to 1 mm), and 100 to 30 mesh (0.15 to 0.6 mm).

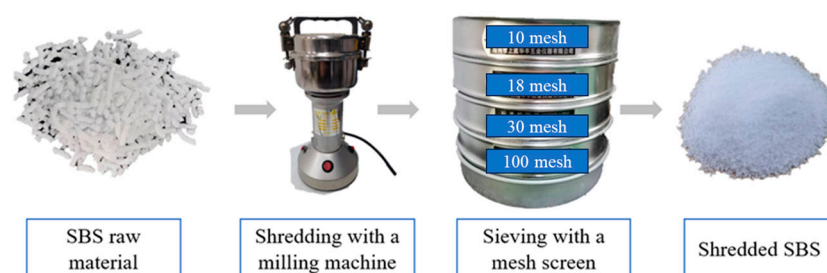


Figure 1. Pre-cutting process of SBS modifier.

2.3. Modified Asphalt Preparation Process

Heat the base asphalt to 160 °C. Gradually add the pre-cut SBS powder into the asphalt in batches until a loading rate of 4.5% is reached. Stir slowly using a glass rod to ensure uniform dispersion. Afterward, add a sulfur-based stabilizer with a loading rate of 0.2%. When the temperature reaches 180 °C, continue stirring at a low speed of 600 r/min.

2.4. Measurement

2.4.1. Laser Confocal Microscopy (LSCM) Test

Microscopic specimens were prepared using the droplet method. A Nikon A1R+ laser (Tokyo, Japan) confocal microscopy system was employed, with the numerical aperture (NA) value set at 1.3 to achieve a resolution of 250 nm. The principle of laser confocal microscopy involves exciting the sample with light of a specific wavelength, inducing fluorescence of a corresponding wavelength. This fluorescence is then observed via conjugate (confocal) detection using illumination pinholes and detection pinholes. The confocal point corresponds to the detected point, and the plane in which the detected point lies is the confocal plane [31].

2.4.2. Conventional Asphalt Tests

The SBS-modified asphalts underwent several standard asphalt tests, including the determination of softening point, penetration, and ductility. The softening points were measured using the ring and ball test method as outlined in GB/T 4507. Penetration tests were conducted at a temperature of 25 °C in accordance with GB/T 4509. Ductility measurements were performed at 5 °C, following the guidelines of GB/T 4508.

2.4.3. Temperature Sweep Test

Temperature sweep testing was conducted following the guidelines of the AASHTO M320 test procedure, with an angular frequency of 10 rad/s and the strain control set at 1%. The temperature range was set at 40 °C to 120 °C, with 10 °C intervals. The rheometer used for these tests was the DHR-3 manufactured by TA Instruments. A 25 mm rotor with a 1 mm gap was chosen for the measurements. At least two parallel tests were performed, and the average value was recorded as the result [32,33].

2.4.4. MSCR Test

The MSCR test is primarily designed to evaluate the performance of modified asphalt at high temperatures [34–36]. In this research, a DHR-3 dynamic shear rheometer from TA Instruments (New Castle, DE, USA) was used and the test was conducted according to AASHTOM 332. Each cycle consisted of 1 s of creep and 9 s of recovery. To mimic high-stress and high-temperature field conditions, only the data obtained at 3.2 kPa and at temperatures ranging from 76 °C to 82 °C were analyzed. R and J_{nr} were calculated, respectively, using Formulas (1) and (2):

$$R\% = \frac{\varepsilon_p - \varepsilon_u}{\varepsilon_p} \times 100\% \quad (1)$$

$$J_{nr} = \frac{\varepsilon_u}{\sigma} \quad (2)$$

where ε_p is the peak strain at 1 s in each cycle; ε_u is the unrecovered strain at 10 s in each cycle; and σ is the creep stress.

2.4.5. LAS Test

The LAS test can be used to evaluate the fatigue performance of asphalt [37]. This research used a DHR-3 dynamic shear rheometer from TA Instruments, and tests were conducted in accordance with the AASHTO TP 101-12-UL specifications. The LAS test protocol consists of two steps. In the first step, the intact rheological properties are measured, and in the second step, the damaged properties of the asphalt are measured. Fatigue life (N_f) at 5% and 15% strain levels can be calculated using Formula (3).

$$N_f = A (\gamma_{max})^{-B} \quad (3)$$

where the coefficients A and B depend on the material properties calculated using the simple viscoelastic continuous loss theory (S-VECD). γ_{max} is the maximum binding deformation expected for a given packaging structure.

2.4.6. BBR Test

This study employed the TE-BBR bending beam rheometer produced by Cannon, a U.S.-based company. The bending creep test for asphalt materials was conducted in accordance with the requirements outlined in the AASHTO T313 specifications. The test temperatures were set at $-12\text{ }^{\circ}\text{C}$ and $-18\text{ }^{\circ}\text{C}$. Within the Superpave design system and its specifications, the stiffness modulus (S) and creep rate (m) values at 60 s from the test results were used as evaluation criteria to assess the low-temperature cracking performance of the asphalt binders [38,39].

2.4.7. Fourier-Transform Infrared (FTIR) Spectroscopy

In the process of swelling and thermal aging, the chemical bonds and molecular structure of modified asphalt change, leading to changes in the peak absorbance and transmission intensity level in the infrared spectrum. This property can be used to determine the degree of aging and the modification effect of modified asphalt.

For this study, a Thermo Scientific™ (Waltham, MA, USA) Nicolet™ iS20 FTIR spectrometer was selected and ATR spectroscopy was used for testing. The wave number range was $4000\sim 600\text{ cm}^{-1}$ for semi-quantitative analysis. I_{Ar} was used to semi-quantitatively analyze the aromatic content of asphalt. I_{PB} and I_{PS} were used to semi-quantitatively analyze the peak areas of polystyrene and polybutadiene, respectively. $I_{C=O}$ was used to characterize the degree of thermal oxygen aging of the modified asphalt. The characteristic parameters of the semi-quantitative analyses were calculated as shown in Formula (4) to Formula (7)

$$I_{PS} = \frac{A_{699}}{\sum A} \times 10000 \quad (4)$$

$$I_{PB} = \frac{A_{966}}{\sum A} \times 10000 \quad (5)$$

$$I_{Ar} = \frac{A_{1600}}{\sum A} \times 10000 \quad (6)$$

$$I_{C=O} = \frac{A_{1700}}{\sum A} \times 10000 \quad (7)$$

where A_{699} , A_{966} , A_{1600} , and A_{1700} = areas of the 699, 966, 1600, and 1700 cm^{-1} spectral bands, respectively; $\sum A$ = sum of the areas between the 600 and 2000 cm^{-1} spectral bands.

2.4.8. Laboratory Binder Aging

According to the rolling thin-film oven test (RTFOT) method (ASTM D2872), short-term aging was performed on the SBS-modified asphalt. A 50 g measure of asphalt was placed in an aging bottle and heated continuously at $163\text{ }^{\circ}\text{C}$ for 85 min.

3. Results and Discussion

3.1. Effect of Mixing Time on the Morphology and Performance of Pre-Cut SBS-Modified Asphalt

For a lateral comparison of the effect of mixing time on the morphology and performance of asphalt prepared with a shredded modifier, this section of the study employed SBS-modified asphalt prepared with an SBS particle size of 30 to 18 mesh (0.6~1 mm). The mixing times were set at 15, 30, 60, and 120 min.

3.1.1. LSCM Test

Laser confocal microscopy experiments were conducted on pre-cut SBS-modified asphalt samples mixed for different amounts of time. The microscopic morphology was observed, and the experimental results are presented in Figure 2.

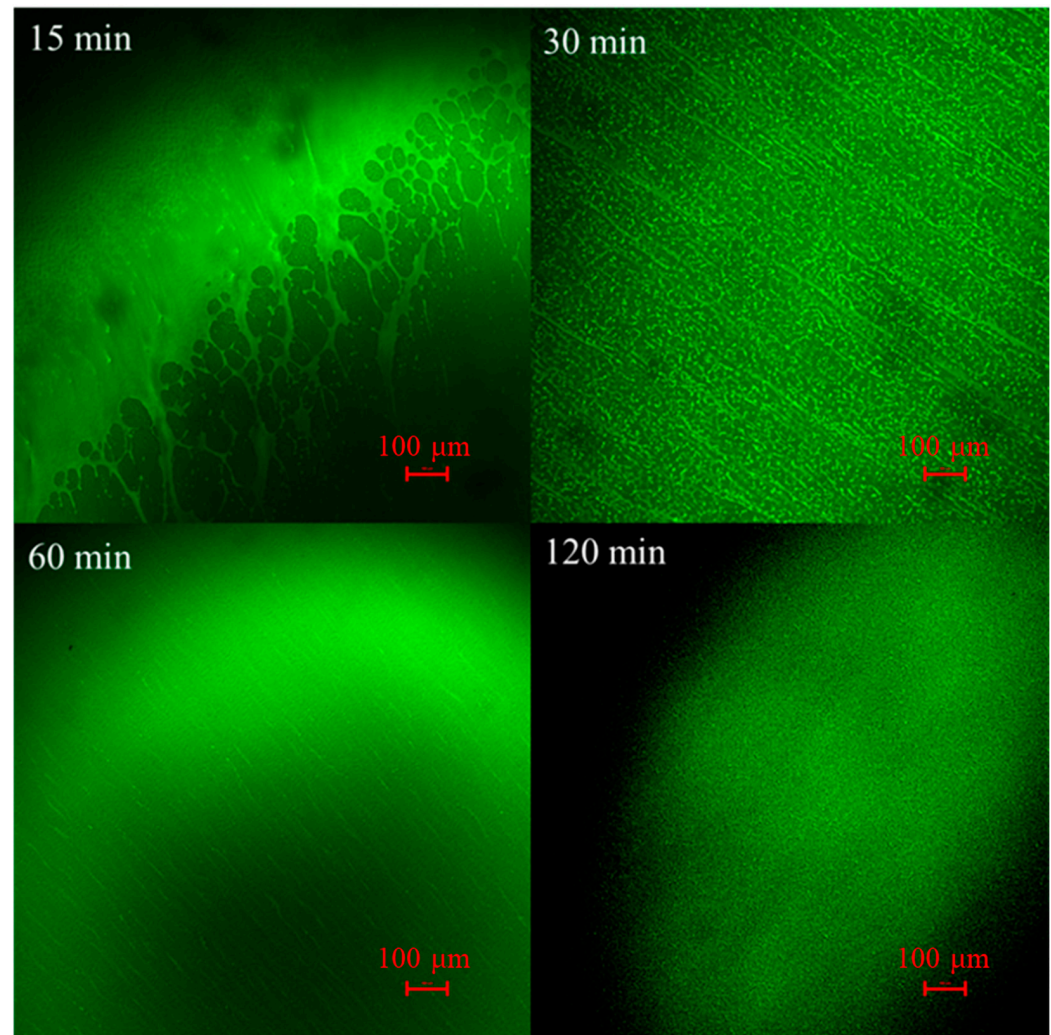


Figure 2. Laser confocal micrographs of pre-cut SBS-modified asphalt mixed for different amounts of time.

The process of morphological change of the SBS modifier in asphalt after mixing was observed. After 15 min of mixing, the particle size of the SBS-modified asphalt was still large, exceeding the display range of the laser confocal microscope. The areas in which SBS came into contact with the asphalt exhibited reticular, filamentous, and punctate patterns. After 30 min of mixing, the particle size of the SBS significantly decreased, and the morphology of the SBS appeared filamentous and punctate within the observation range of the laser confocal microscope. As the mixing continued, at 60 min, the SBS morphology remained filamentous and punctate. However, compared to the 30 min mark, the filaments were narrower and the punctate particles were smaller. Additionally, some filamentous SBS particles exhibited a trend towards becoming punctate. After 120 min of mixing, the SBS morphology had transformed completely into a punctate form.

The glass transition temperature of polystyrene ranges from 80 °C to 105 °C, while the glass transition temperature of polybutadiene is around −15 °C. In star-shaped SBS, the polystyrene phase is dispersed as spherical domains within the continuous polybutadiene phase and the polystyrene domains are interconnected directly [40]. It can be assumed

that during the heat absorption process of SBS, a phase transition will occur first in the portions with higher contents of polybutadiene, while the parts with higher contents of polystyrene will not undergo a phase transition at this point. Based on these considerations and the morphological changes of the SBS during the mixing process, this study produced speculations about the changes in SBS during the preparation process, as illustrated in Figure 3.

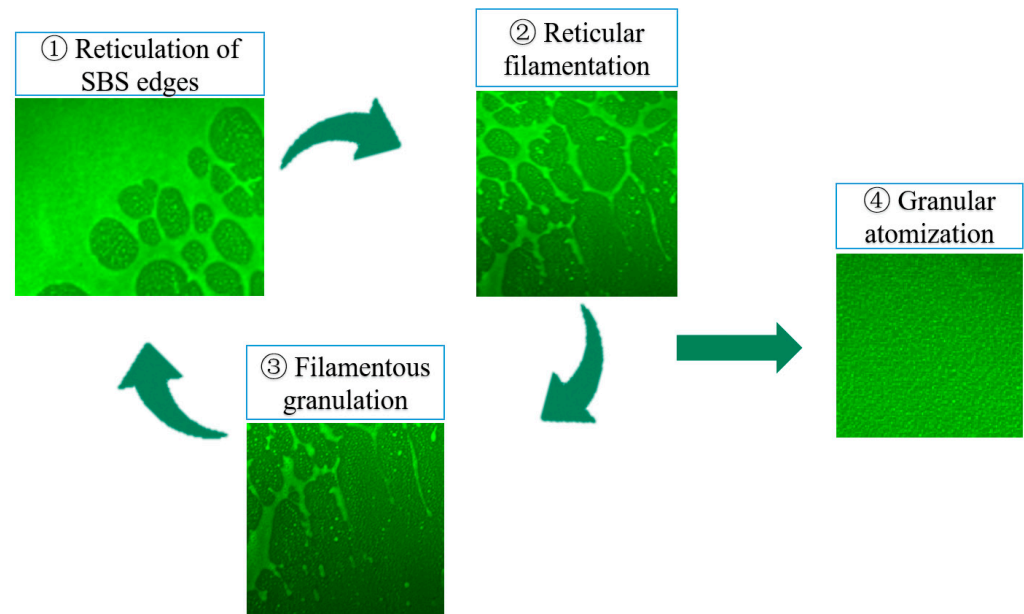


Figure 3. Morphological transformation process of shredded modifier during mixing.

- (1) Reticulation of SBS edges: After coming into contact with asphalt, the edges of the SBS, being the first parts to make contact with the high-temperature asphalt, absorb heat initially. When a certain amount of heat has been absorbed, the portions with higher contents of polybutadiene undergo a phase transition, leading to the formation of voids along the edges of the SBS. However, the parts with higher contents of polystyrene do not yet undergo a phase transition, resulting in the formation of a reticular structure.
- (2) Reticular filamentation: The reticular structure continues to absorb heat from the high-temperature asphalt. In the connecting region between two areas with higher polystyrene contents, the glass transition temperature is lower than that of the high-polystyrene-content part. This causes a phase transition in the connecting regions, leading to the disruption of the reticular structure and its transformation into a filamentous one.
- (3) Filamentous granulation: The filamentous structure absorbs heat from the high-temperature asphalt. In the edges and some internal areas of the filamentous structure, where the polystyrene content is relatively lower, phase transitions are more likely to occur. As a result, filaments break off from the edges or interior, forming granules with relatively higher polystyrene contents.
- (4) Granular atomization: The granular SBS structure continues to absorb heat, repeating the aforementioned morphological changes. With each iteration of the reticular, filamentous, and granular transformations, the particle size of the SBS significantly reduces. After undergoing several cycles of these changes, the diameter of the SBS particles approaches the resolution of the laser confocal microscope, visually presenting an atomization effect.

3.1.2. Conventional Asphalt Tests

Conventional asphalt tests were conducted on pre-cut SBS-modified asphalt mixed for varying amounts of time, and the results of these tests are presented in Figure 4.

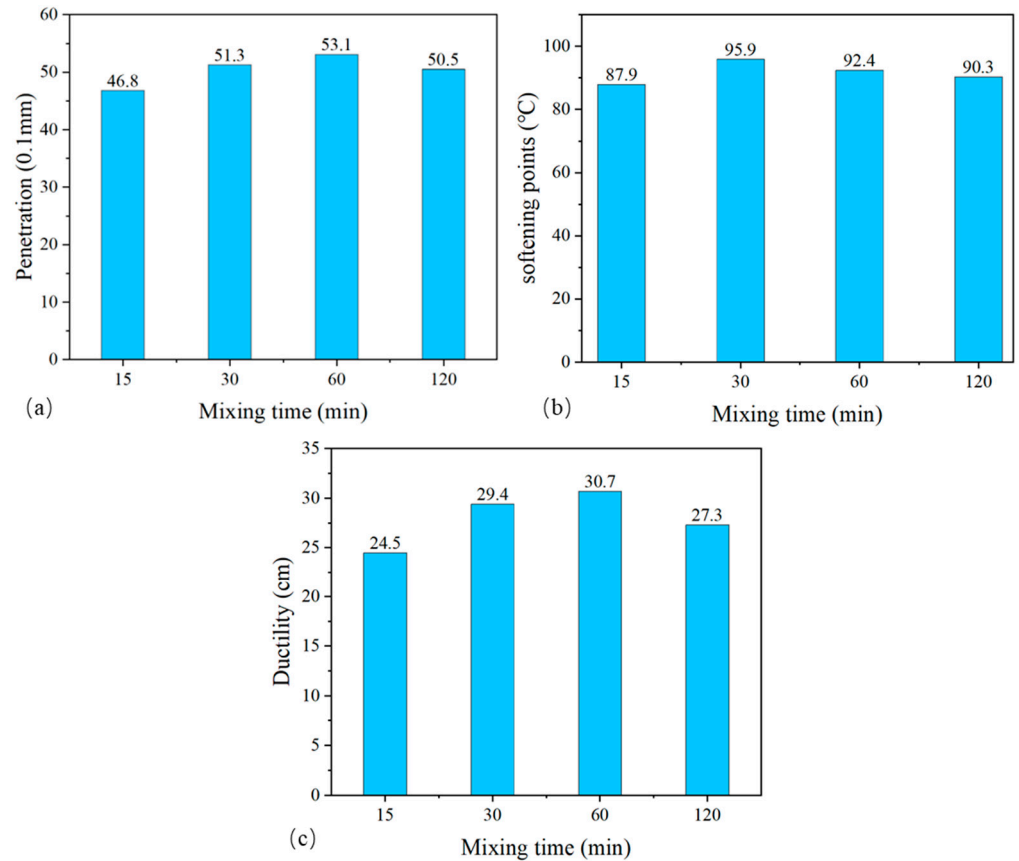


Figure 4. Results of the conventional asphalt tests of pre-cut SBS-modified asphalt mixed for different amounts of time. (a) Penetration; (b) softening point; (c) ductility.

Penetration increased initially and then decreased as mixing time increased. After 15 min of mixing, the SBS morphology displayed larger particles, leading to higher asphalt hardness. After 30 and 60 min of mixing, the SBS morphology transformed into filamentous and aggregated particles, resulting in reduced asphalt hardness. After 60 min, the narrower filaments and smaller particle diameters led to even lower asphalt hardness, hence the increase in penetration. However, after 120 min, the SBS morphology displayed foggy particles, increasing the hardness and decreasing the penetration.

The softening point showed an initial increase and subsequent decrease with mixing time. After 15 min of mixing, the SBS morphology with larger particles formed a weaker network structure, resulting in the lowest softening point. After 30 min of mixing, the SBS morphology transformed into filamentous and aggregated particles, enhancing the network structure's strength and causing the softening point to rise. After 60 min of mixing, the reduction in filament width and particle diameter weakened the network structure, leading to a decrease in softening point. After 120 min of mixing, the foggy particles in the SBS further weakened the network structure, leading to a continued decrease in the softening point.

Ductility increased initially and then decreased with mixing time. After 15 min of mixing, the SBS morphology with larger particles formed a weaker network structure, resulting in the lowest ductility. After 30 min of mixing, the SBS morphology transformed into filamentous and aggregated particles, enhancing the asphalt's extensibility and leading to increased ductility. After 60 min, the SBS morphology remained filamentous and

aggregated, and the narrower filaments and smaller particle diameters further enhanced the asphalt's extensibility, causing ductility to further increase. However, after 120 min, the foggy particles in the SBS weakened the network structure further, causing a decrease in ductility.

3.1.3. Temperature Sweep Test

Temperature sweep tests were conducted on pre-cut SBS-modified asphalt samples mixed for different amounts of time. The experimental results are presented in Figure 5.

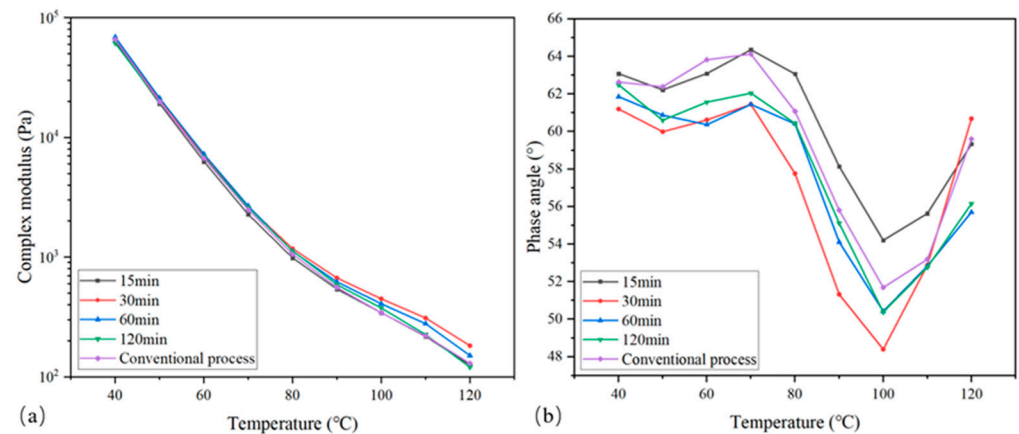


Figure 5. Temperature sweep test of pre-cut SBS-modified asphalt mixed for different amounts of time. (a) Complex modulus, (b) phase angle.

When mixed for 15 min, the complex modulus of the pre-cut SBS-modified asphalt was lower than that of the conventional-process asphalt and the phase angle was greater, indicating that the modification effect at this point was not significant and the proportion of viscosity in the modified asphalt was higher. This can be attributed to insufficient blending of the SBS modifier agent and the asphalt due to the larger particle size of the SBS in this state and the short mixing time.

After 30 min of mixing, the complex modulus of the pre-cut SBS-modified asphalt significantly increased and surpassed that of the conventional-process asphalt. The phase angle was also notably smaller, indicating a substantial enhancement in the modification effect. A higher complex modulus and a smaller phase angle led to a larger rutting factor and better resistance to rutting deformation. This can be attributed to the filamentous and granular structure of the SBS in this state, which increased the interlocking effect of the SBS and enhanced the strength of the spatial network structure.

After 60 min of mixing, the complex modulus of the pre-cut SBS-modified asphalt slightly decreased compared to that assessed at the 30 min mark and the phase angle increased, suggesting a minor reduction in the resistance to rutting and an increase in the proportion of viscosity. This was due to the narrower filamentous structure and smaller particle diameter, which weakened the strength of the network structure.

After 120 min of mixing, the complex modulus of the pre-cut SBS-modified asphalt decreased further and the phase angle continued to increase, indicating a further weakening of the high-temperature performance, though it remained better than that of the conventional-process asphalt. This was due to the atomized particle form of SBS at this stage, which weakened the strength of the network structure. This implies that an excessively long mixing time is not advisable.

3.1.4. MSCR Test

MSCR tests were conducted on pre-cut SBS-modified asphalt samples mixed for different amounts of time. The experimental results are presented in Figure 6.

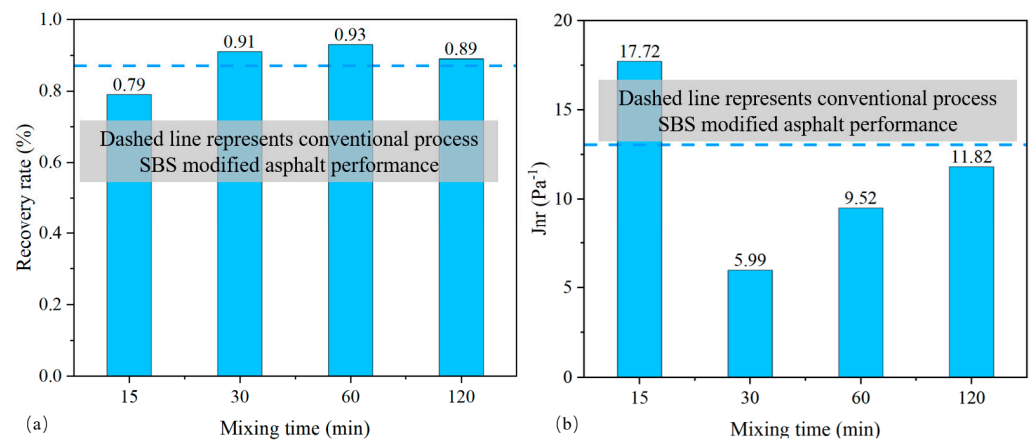


Figure 6. MSCR test of pre-cut SBS-modified asphalt mixed for different amounts of time. (a) Recovery rate, (b) Jnr.

The rutting recovery rate is related to deformation recovery capability. In Figure 6a, it can be observed that the rutting recovery rate of the pre-cut SBS-modified asphalt mixed for 15 min was weaker than that of the conventionally prepared SBS-modified asphalt. This was attributed to the inadequate mixing of the modifier with the asphalt, resulting in a poor modification effect. However, after mixing for more than 30 min, the rutting recovery rate of the pre-cut SBS-modified asphalt exceeded that of the conventional-process asphalt. This suggests that after mixing for 30 min, the elastic recovery performance of pre-cut SBS-modified asphalt can replace that of conventionally prepared SBS-modified asphalt. When mixed for 30–60 min, longer mixing times resulted in higher rutting recovery rates and stronger deformation recovery capability. This was due to the filamentous structure of the SBS, which increased the interlocking effect and strengthened the spatial network structure. After mixing for 120 min, the rutting recovery rate decreased due to the atomized particle form of the SBS, which weakened the strength of the network structure.

Non-recoverable creep compliance reflects resistance to deformation. In Figure 6b, it can be seen that the non-recoverable creep compliance of the pre-cut SBS-modified asphalt mixed for 15 min was greater than that of the conventional-process asphalt. This indicates that at this stage, SBS was unevenly dispersed with a large particle size, resulting in a poor modification effect due to inadequate mixing with the asphalt. However, after mixing for 30 min, the non-recoverable creep compliance of the pre-cut SBS-modified asphalt was lower than that of the conventional-process asphalt, demonstrating an improved resistance to deformation which surpassed that of the conventional SBS asphalt. However, after 60 min of mixing, the deformation resistance was weaker than that at 30 min, indicating that when SBS is in a filamentous state, smaller filament width and granular diameter lead to poorer deformation resistance. After mixing for 120 min, the deformation resistance was further weakened due to the atomized particle form of SBS.

3.1.5. LAS Test

LAS tests were conducted on pre-cut SBS-modified asphalt samples mixed for different amounts of time. The stress–strain curves are presented in Figure 7.

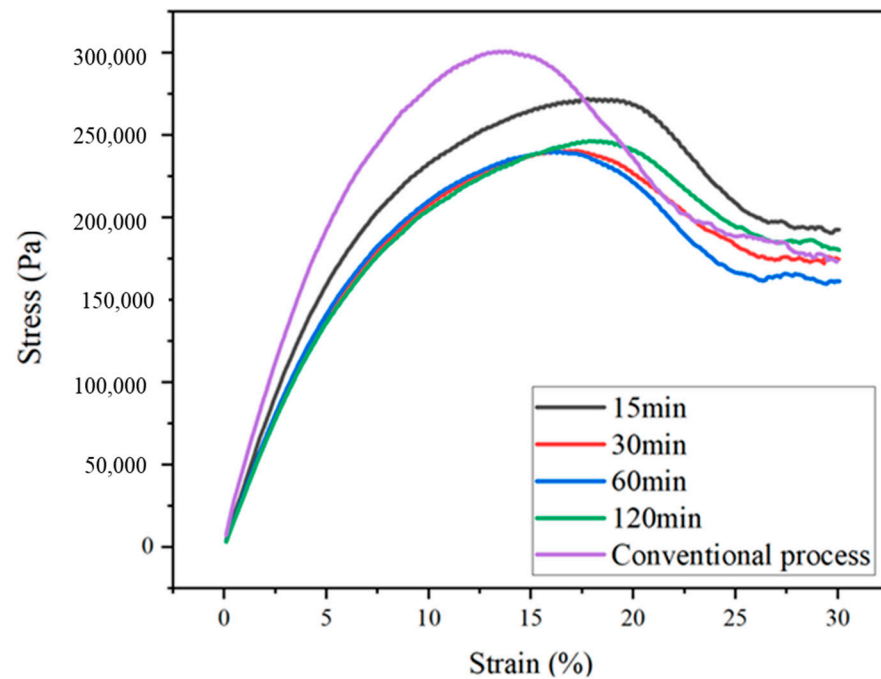


Figure 7. Stress–strain curves of pre-cut SBS-modified asphalt mixed for different amounts of time.

The critical strain is defined at the point at which the stress starts to decrease. Beyond this point, a material's behavior changes, entering the failure stage. It was observed that the critical strain points of the pre-cut SBS-modified asphalt samples were all greater than those of the conventional-process asphalt samples, indicating that pre-cut SBS-modified asphalt can withstand larger strains before fatigue failure. The width of the peak is related to pressure sensitivity, with a wider peak indicating lower pressure sensitivity. It can be seen that the peaks of pre-cut SBS-modified asphalt were wider than those of the conventional-process asphalt. The stress peak values were ordered as follows: conventional process > 15 min > 120 min > 30 min > 60 min. The stress peak represents the hardness of asphalt. The stress peaks of the pre-cut SBS-modified asphalt were lower than those of the conventional-process asphalt. This is because pre-cutting increased the surface area of the SBS, resulting in larger contact area with the base asphalt. This increased contact area facilitated swelling, leading to reduced hardness and enhanced flexibility of the modified asphalt. Within the mixing time range of 15 to 60 min, longer mixing times resulted in smaller stress peaks and greater flexibility of the modified asphalt, indicating that a 60 min mixing time yielded the best swelling effect of the pre-cut SBS modifier. However, after mixing for 120 min, the stress peak increased, which may be attributable to prolonged mixing causing changes in the asphalt components.

A steeper slope of the stress peak decrease during the failure stage indicates greater brittleness and susceptibility to damage of the specimen. Similarly, the slopes of peak decrease for pre-cut SBS-modified asphalt were gentler than those of the conventional-process asphalt, indicating that the strain limit during the failure stage was larger for the pre-cut modified asphalt. The steeper slope of the peak decrease for the 60 min mixing group indicates that faster deformation occurred during failure, which was attributed to the narrower filament width and granular diameter.

From the stress–strain curve characteristics, it can be deduced that the fatigue failure characteristics of the pre-cut SBS-modified asphalt were superior to those of the conventional-process asphalt. Furthermore, the calculated fatigue life N_f values for pre-cut SBS-modified asphalt samples prepared with different mixing times are shown in Figure 8.

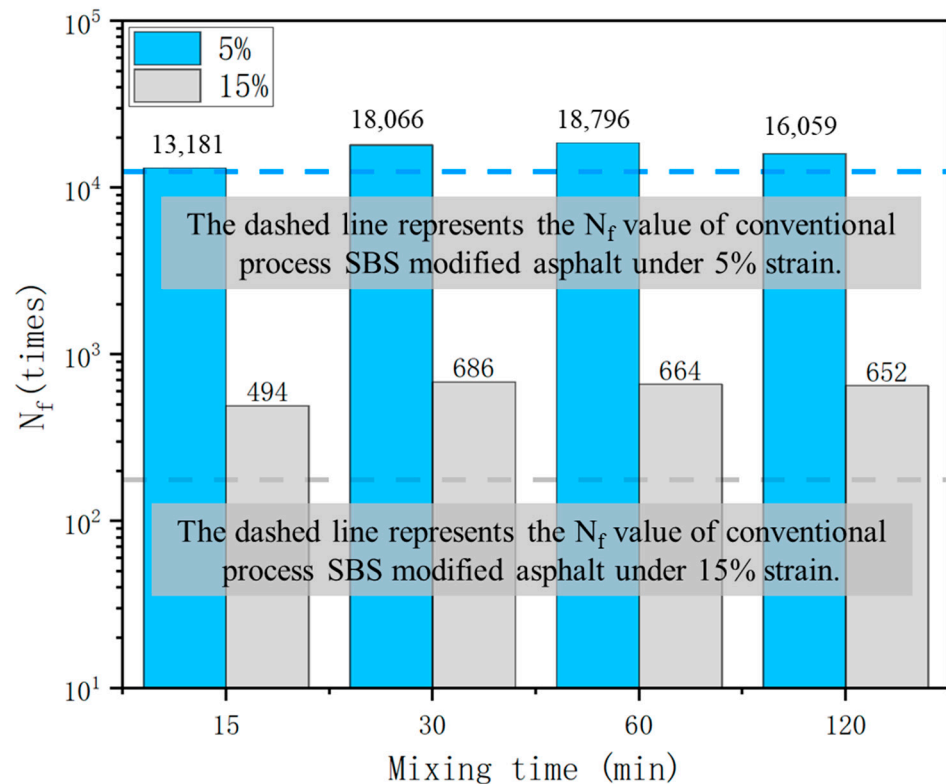


Figure 8. Fatigue life (N_f) values of pre-cut SBS-modified asphalt mixed for different amounts of time.

At both 5% and 15% strain levels, the fatigue life (N_f) values of the pre-cut SBS-modified asphalt were greater than those of the conventional-process asphalt. Under both 5% and 15% strain levels, the fatigue life of the pre-cut SBS-modified asphalt initially increased and then decreased with increasing mixing time. This suggests that when the SBS structure is filamentous and granular, the fatigue life is greater compared to when the SBS structure is particulate or atomized. This is due to the stronger interlocking effect and higher strength of the network structure when SBS is in a filamentous and granular state.

At a 5% strain level, the pre-cut SBS-modified asphalt mixed for 60 min exhibited the maximum fatigue life. This implies that when the strain level is much lower than the critical strain, the fatigue life is related to the characteristics of the asphalt's stress–strain curve in the first half. In this scenario, greater asphalt ductility corresponds to a longer fatigue life.

At a 15% strain level, the pre-cut SBS-modified asphalt mixed for 30 min showed the highest fatigue life. This suggests that when the strain level is close to the critical strain, the fatigue life is related to the characteristics of the asphalt's stress–strain curve in the latter half. In this case, a stronger network structure and larger strain limit during the failure stage lead to a greater fatigue life.

3.1.6. BBR Test

BBR tests were conducted on pre-cut SBS-modified asphalt samples mixed for different amounts of time. The stiffness modulus (S) and m -value results are shown in Figure 9.

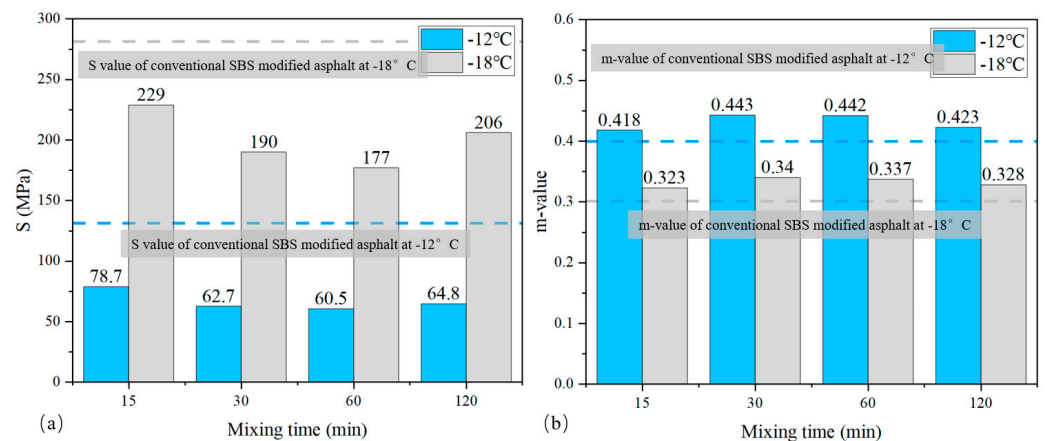


Figure 9. BBR test results of pre-cut SBS-modified asphalt mixed for different amounts of time. (a) Stiffness modulus, (b) m-value.

The stiffness modulus (S) of the pre-cut SBS-modified asphalt was lower than that of the SBS-modified asphalt prepared through the conventional process, and the m -value was larger. This indicates that the pre-cut SBS-modified asphalt, after being shredded, was softer at low temperatures, had greater ductility, and exhibited better stress relaxation capacity. At the testing temperature, when the SBS structure was filamentous and granular, the stiffness modulus was smaller compared to when the SBS structure was particulate or atomized, while the m -value showed the opposite trend. This suggests that low-temperature crack resistance is better when the SBS structure is filamentous and granular. The lower stiffness modulus after 60 min of mixing compared to 30 min indicates that a narrower filament width and smaller granular diameter resulted in greater asphalt ductility. The larger m -value at 30 min of mixing compared to 60 min indicates that a wider filament width and larger granular diameter led to stronger stress relaxation capacity.

3.2. Effect of Shredded Particle Size on Microscopic Morphology and Performance of Pre-Cut SBS-Modified Asphalt

In the aforementioned study, it was observed that pre-cut SBS-modified asphalt with a mixing time of over 30 min exhibited superior rheological performance compared to conventionally prepared SBS-modified asphalt. Therefore, to investigate the effects of shredded particle size on the physicochemical characteristics, morphology, and performance of pre-cut SBS-modified asphalt, samples were prepared by low-speed mixing for 30 min using three different particle sizes of pre-cut SBS (10-18 mesh, 18-30 mesh, 30-100 mesh).

3.2.1. LSCM Test

Laser confocal microscopy experiments were conducted on SBS-modified asphalt samples with different pre-cut particle sizes to observe their microscopic morphology. The test results are presented in Figure 10.

In the pre-cut SBS-modified asphalt with a particle size of 18-10 mesh, the morphology of the SBS modifier was similar to that in the conventional-process asphalt. Clear SBS particles were observed, but the maximum particle size was smaller than that of the conventional-process asphalt. In the 18-10 mesh SBS-modified asphalt, the SBS particles mostly exhibited a granular distribution with varying sizes, and some smaller particles showed a tendency toward filamentous distribution. In the pre-cut SBS-modified asphalt with a particle size of 30-18 mesh, the SBS particles mostly exhibited a filamentous distribution, with a few appearing as small granular shapes. In the case of the 100-30 mesh SBS-modified asphalt, the SBS morphology included partially filamentous distribution, but with shorter lengths; some particles were in the form of small granules, and there were even extremely small particles that visually resembled a hazy mist.

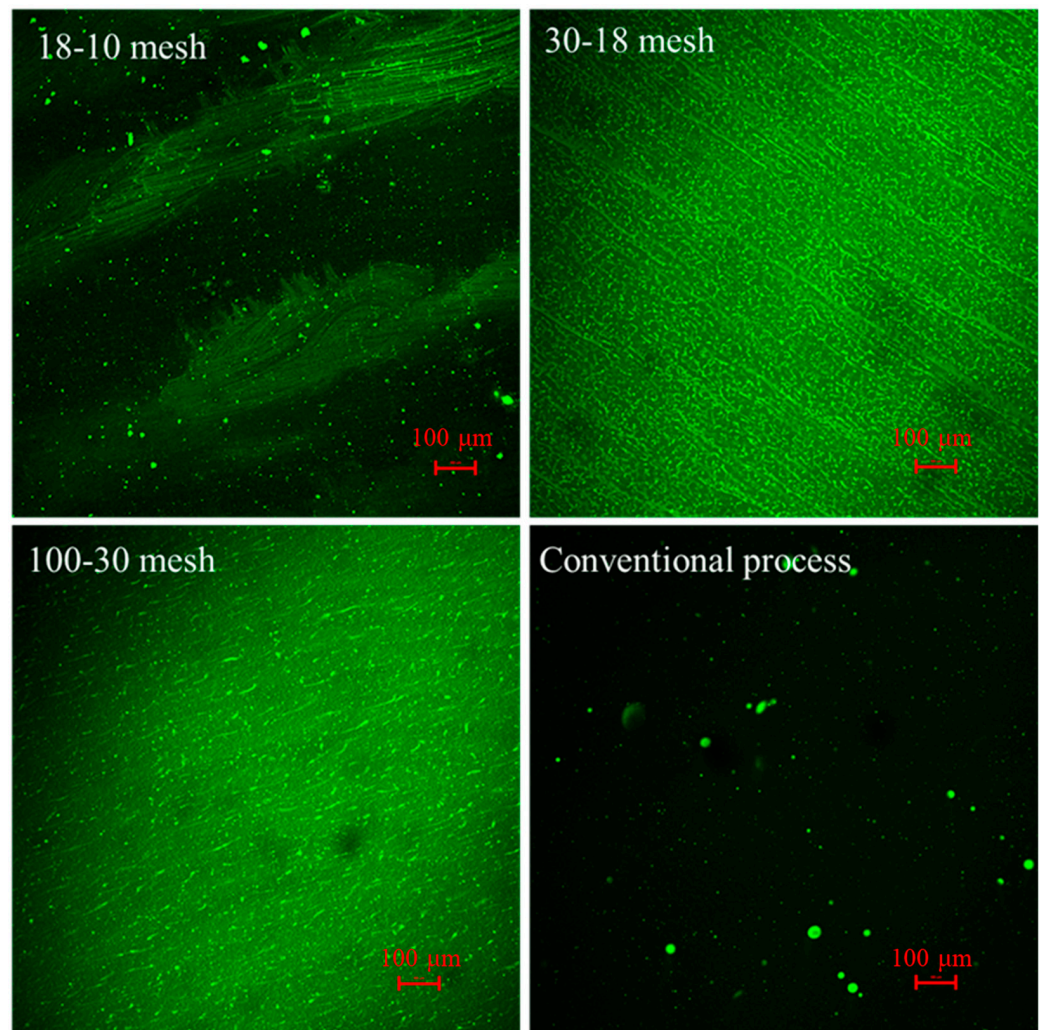


Figure 10. Laser confocal microscopic images of modified asphalt with different shredded particle sizes.

According to the morphological transformation process of SBS described in Section 3.1, the conventional process produces SBS-modified asphalt with the fewest cycles of morphological changes, which is why larger SBS particles were still present. The 18-10 mesh SBS underwent a slightly higher number of morphological change cycles, resulting in noticeable SBS particles. The 30-18 mesh and 100-30 mesh SBS underwent even more cycles. This suggests that when preparing modified asphalt through the mixing process, smaller pre-cut SBS particle sizes undergo more cycles of morphological changes. The higher number of cycles for pre-cut SBS-modified asphalt indicates increased contact area with the asphalt, higher heat absorption, and an enhanced blending effect with the asphalt. Based on the microscopic morphology of the SBS-modified asphalt, it can be inferred that pre-cut SBS effectively replaced the high-shear mixing process.

3.2.2. Conventional Asphalt Tests

Conventional asphalt tests were conducted on pre-cut SBS-modified asphalt with different particle sizes, and the results of these tests are presented in Figure 11.

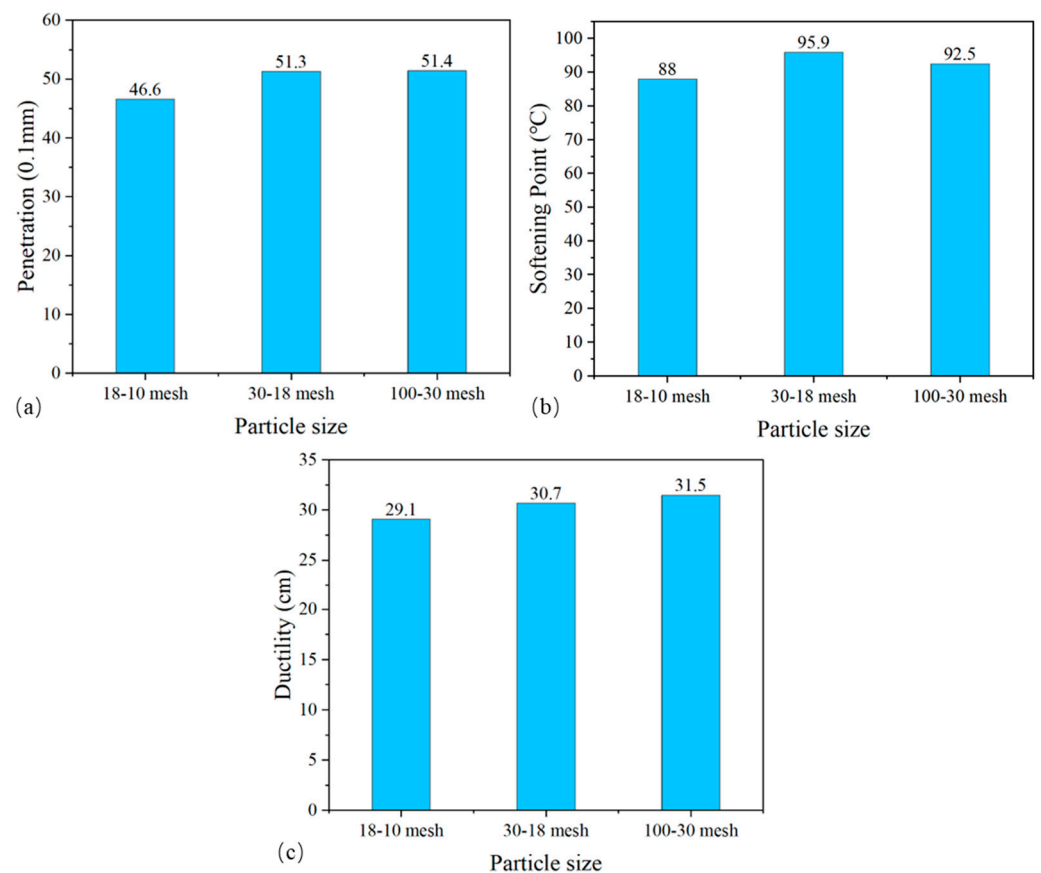


Figure 11. Conventional asphalt tests of SBS-modified asphalt with different pre-cut particle sizes. (a) Penetration; (b) softening point; (c) ductility.

As the pre-cut particle size of SBS decreased, the penetration of the modified asphalt increased and the hardness gradually decreased. In particular, the modified asphalt with an 18-10 mesh particle size exhibited significantly lower penetration and higher hardness. This indicates that the transition of SBS morphology from the stage where particles were clearly observed to the filamentous and aggregated stage led to a substantial reduction in hardness. Furthermore, in the filamentous and aggregated stage, as the number of cycles increased, smaller filament widths and particle diameters contributed to lower asphalt hardness. This is because when SBS is in a state of particle morphology, the three-dimensional network structure of the polymer provides greater hardness, whereas in the filamentous and aggregated stage, this network structure's hardness diminishes.

As the pre-cut particle size of the SBS decreased, the softening point of the modified asphalt initially increased and then decreased. The modified asphalt with a 30-18 mesh particle size demonstrated the highest softening point, followed by the modified asphalt with a 100-30 mesh particle size, and the modified asphalt with an 18-10 mesh particle size exhibited the lowest softening point. The tests indicated that when the SBS morphology transitioned from the particle stage to the filamentous and aggregated stage, the softening point of the modified asphalt increased. This is because in the filamentous and aggregated stage, the filamentous SBS is more prone to tangling and knotting, resulting in more significant spatial hindrance. Moreover, excessively small filament widths and particle diameters can weaken the extent of tangling, leading to a decrease in the softening point.

As the pre-cut particle size of SBS decreased, the ductility of the modified asphalt gradually increased, indicating improved extensibility. This implies that the transition of SBS morphology from the stage where particles were clearly observed to the filamentous and aggregated stage enhanced the extensibility. Additionally, in the filamentous and aggregated stage, as the number of cycles increased, smaller filament widths and particle

diameters contributed to stronger asphalt extensibility. In contrast to the softening point, when the SBS morphology shifted from the particle stage to the filamentous and aggregated stage, the three-dimensional polymer network structure's hardness was diminished. However, an enhancement of extensibility arose from the entanglement of filamentous SBS in this stage.

3.2.3. Temperature Sweep Test

Temperature sweep tests were conducted on pre-cut SBS-modified asphalt with different shredded particle sizes. The experimental results are shown in Figure 12.

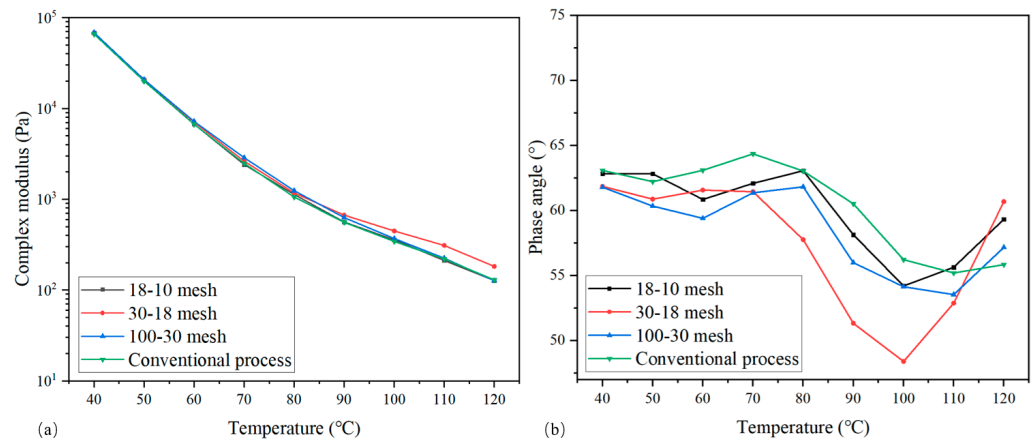


Figure 12. Temperature sweep tests of modified asphalt with different shredded particle sizes. (a) Complex modulus, (b) phase angle.

In Figure 10a, it can be observed that the complex modulus of SBS-modified asphalt prepared by different shredded particle sizes through mixing was consistently higher than that of the conventional-process asphalt at each scanning temperature. Among the samples, the complex modulus of the asphalt with shredded particles sized 30-18 mesh was the highest, followed by 100-30 mesh, and that for 18-10 mesh was the lowest. The results indicate that the complex modulus was greater when the SBS was in a fibrous and particulate combination state as opposed to a predominantly granular state. This is attributed to the higher intertwining of the fibrous morphology, which led to a more intricate spatial network structure that enhanced its load-bearing capacity at elevated temperatures. Furthermore, in the fibrous and particulate combination state, as the width of the fibrous elements and the diameter of the particulates decreased, the strength of the interwoven spatial network structure diminished.

In Figure 10b, it is evident that the phase angle of the SBS-modified asphalt prepared with different shredded particle sizes was generally lower than that of the conventional-process asphalt, indicating a higher elastic proportion in the pre-cut SBS-modified asphalt. Among the three different shredded particle sizes prepared through mixing, the asphalt with shredded particles sized 30-18 mesh exhibited the smallest phase angle, followed by 100-30 mesh, and the 18-10 mesh exhibited the largest phase angle. This trend can also be attributed to the fibrous morphology of the SBS. The interlocking nature of the fibrous SBS enhanced the elasticity of the network structure. Additionally, the wider fibrous elements contributed to a stronger network structure, resulting in greater elasticity.

3.2.4. MSCR Test

The experimental results of the MSCR tests conducted on pre-cut SBS-modified asphalt with different shredded particle sizes are shown in Figure 13.

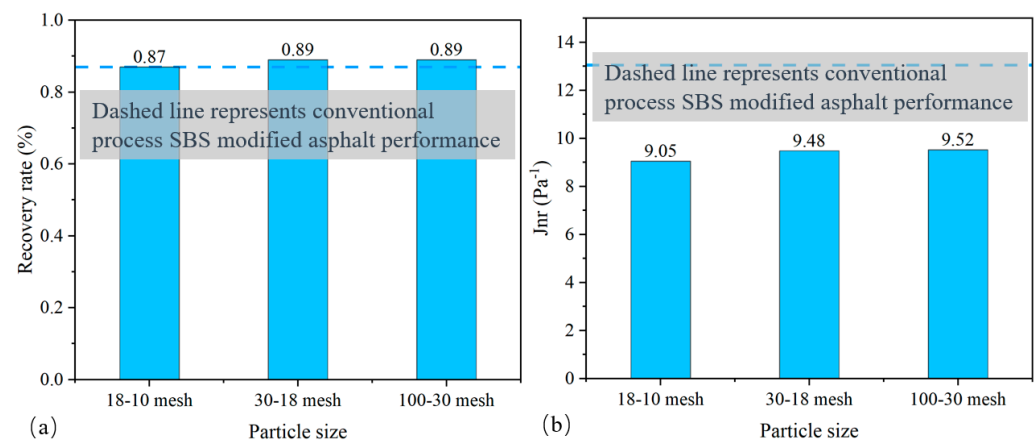


Figure 13. MSCR tests on modified asphalt mixed with different shredded particle sizes. (a) Recovery rate, (b) Jnr.

In Figure 13a, it can be observed that the creep recovery rates of SBS-modified asphalt samples prepared by mixing with different shredded particle sizes were all greater than those of the conventional-process asphalt samples. This indicates that the pre-cut SBS-modified asphalt had a stronger elastic recovery capability. Among the three different shredded particle sizes, the rates of the 30-18 mesh and 100-30 mesh samples were greater than those of the 18-10 mesh samples. The test showed that SBS-modified asphalt containing fibrous morphology had a stronger elastic deformation recovery capability, which was attributed to the easier intertwining of fibrous SBS-modified asphalt, which enhanced the elastic deformation recovery capability of the modified asphalt.

In Figure 13b, it can be seen that the non-recoverable creep stiffness of the SBS-modified asphalt prepared by mixing with different shredded particle sizes was smaller than that of the conventional-process asphalt. This indicates that the pre-cut SBS-modified asphalt had a stronger resistance to deformation. Among the three different shredded particle sizes, the non-recoverable creep stiffness of the 18-10 mesh was the smallest, followed by the 100-30 mesh, and that of the 30-18 mesh was the largest. The test showed that SBS-modified asphalt with obvious granular morphology had a stronger resistance to deformation. This is because the advantages of the network structure formed by granular structures of SBS are reflected in terms of strength. When the SBS morphology is a combination of fibrous and granular shapes, the larger the width of the fibrous structure and the diameter of the granular structure, the stronger the network structure strength and the stronger the resistance to deformation.

3.2.5. LAS Test

The stress–strain curves of pre-cut SBS-modified asphalt with different shredded particle sizes were assessed using the LAS test. The results are shown in Figure 14.

The stress peak values of SBS-modified asphalt prepared by mixing with different shredded particle sizes were smaller than those of the conventional-process asphalt, and the critical strain points and peak width were larger than those of the conventional-process asphalt. This indicates that the pre-cut SBS-modified asphalt had greater ductility and lower stress sensitivity at elevated temperatures, and entered the failure stage later. The experiment showed that when the SBS structure was predominantly granular, the smaller the particle diameter, the smaller the stress peak value and the lower the asphalt hardness. When the SBS structure transitioned from predominantly granular to filamentous with granules, the stress peak value was further reduced, resulting in even lower asphalt hardness. However, as the filament width and particle diameter decreased, the critical strain point further increased, enhancing the limit of failure.

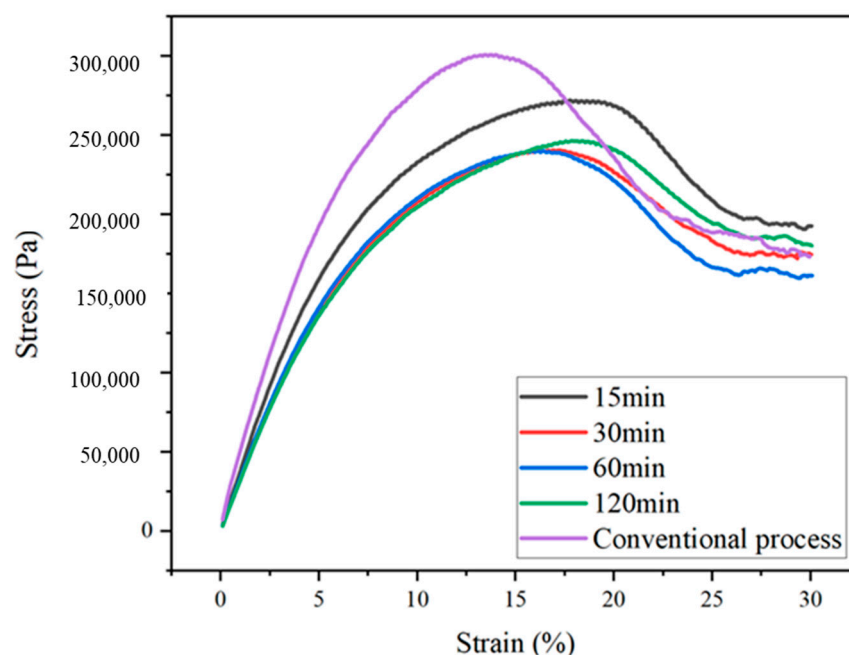


Figure 14. Stress–strain curves of modified asphalt mixed with different shredded particle sizes.

During the failure stage, a steeper slope of the peak decrease indicates greater brittleness of the specimen and easier damage. The conventional process for SBS-modified asphalt exhibited the steepest peak decrease slope, leading to rapid failure. Although the structure of asphalt prepared with SBS with a particle size of 18–10 mesh was similar to that of the conventional-process asphalt, the slope of the peak decrease was significantly smaller. This implies that when the SBS structure was granular, a smaller particle diameter resulted in reduced brittleness during the failure stage and longer fatigue life. The modified asphalt samples with particle sizes of 30–18 mesh and 100–30 mesh had both filamentous and granular SBS structures. However, the slope of the peak decrease for the 30–18 mesh asphalt was noticeably smaller, indicating that larger filament width and particle diameter led to reduced brittleness during the failure stage.

Furthermore, the calculated fatigue life N_f values of pre-cut SBS-modified asphalt samples mixed for different mixing times are shown in Figure 15.

At 5% and 15% strain levels, the N_f values of SBS-modified asphalt samples mixed with different shredded particle sizes were all greater than those of the conventional-process asphalt samples. This indicates that the pre-cut SBS-modified asphalt prepared through mixing exhibited excellent intermediate temperature fatigue performance. Under the 5% strain condition, as the shredded particle size decreased, the fatigue life of the pre-cut SBS-modified asphalt continued to increase. This phenomenon can be attributed to the fact that at low strain levels, the critical failure strain is not reached and the modified asphalt retains its higher ductility, resulting in an extended fatigue life.

Under the 15% strain condition, the fatigue life of the pre-cut SBS-modified asphalt first increased and then decreased as the shredded particle size decreased. Among the different shredded particle sizes, the modified asphalt with a shredded particle size of 30–18 mesh had the maximum fatigue life, followed by 18–10 mesh, and the smallest value was observed for 100–30 mesh. This behavior was observed because the 15% strain level was close to the critical failure strain, at which point the three-dimensional network structure strength of a modified asphalt becomes a crucial parameter in determining its fatigue life. The fatigue life of modified asphalt is jointly determined by its ductility and the strength of the three-dimensional network structure. The network structure of the 100–30 mesh asphalt, due to the smaller filament width and particle diameter, had a weaker load-carrying capacity compared to 30–18 mesh, leading to a shorter fatigue life under high strain levels. On the other hand, the modified asphalt with a shredded particle size of

30-18 mesh possessed a balanced combination of ductility and three-dimensional network structure strength, resulting in the highest fatigue life. Although the modified asphalt with a shredded particle size of 18-10 mesh had a robust network structure, its slightly lower ductility resulted in a slightly lower fatigue life compared to the 30-18 mesh case.

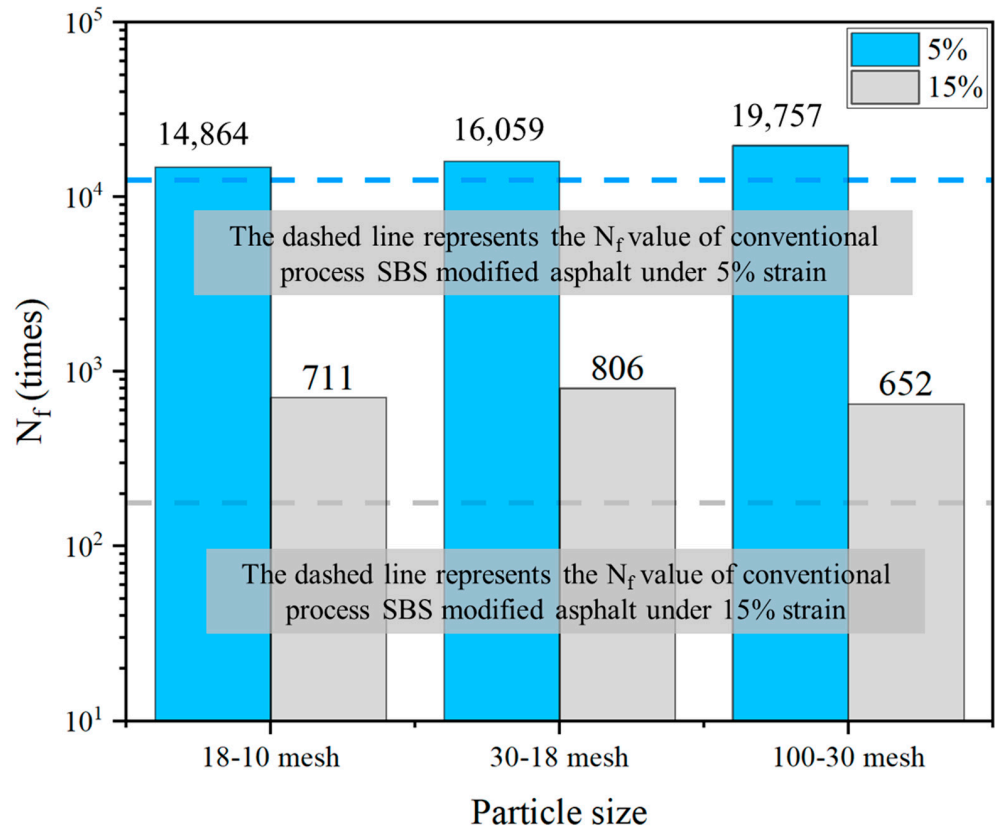


Figure 15. Fatigue life (N_f) of modified asphalt mixed with different shredded particle sizes.

3.2.6. BBR Test

BBR tests were conducted on pre-cut SBS-modified asphalt with different shredded particle sizes. The experimental outcomes are depicted in Figure 16.

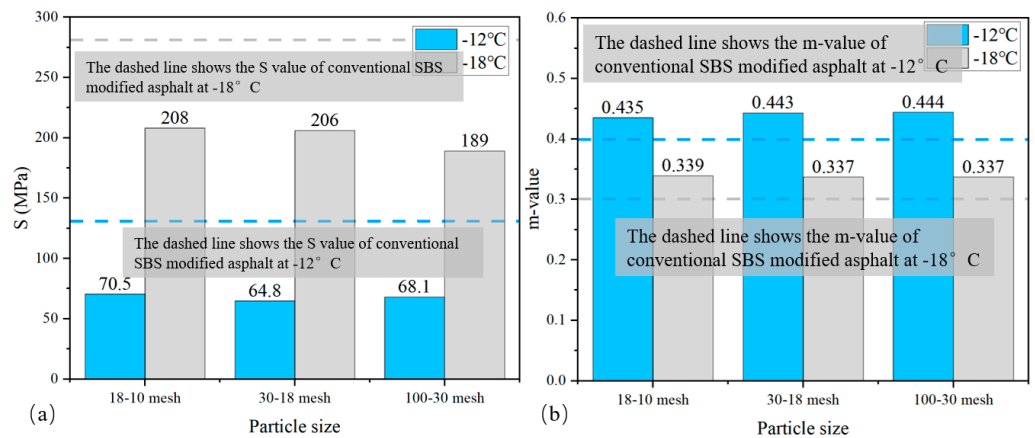


Figure 16. BBR tests on modified asphalt mixed with different shredded particle sizes. (a) Stiffness modulus, (b) m-value.

The stiffness modulus of the SBS-modified asphalt with different shredded particle sizes was lower than that of the SBS-modified asphalt prepared by conventional methods.

This indicates that the SBS-modified asphalt that underwent shredding was softer and more ductile at low temperatures, demonstrating excellent resistance to cracking. At both test temperatures, smaller shredded particle sizes of SBS resulted in a lower stiffness modulus and greater ductility. This suggests that SBS with filamentous and punctate morphology, especially when narrower, exhibits better low-temperature cracking resistance. This conclusion aligns with the findings of the study on the effect of mixing time.

Similarly, the m -values of the SBS-modified asphalt samples with different shredded particle sizes were also higher than those of the SBS-modified asphalt samples prepared conventionally, indicating that the stress relaxation ability of the pre-shredded SBS-modified asphalt was better. At $-12\text{ }^{\circ}\text{C}$, smaller shredded particle sizes of SBS corresponded to higher m values, indicating stronger stress relaxation capacity. However, at $-18\text{ }^{\circ}\text{C}$, smaller shredded particle sizes of SBS resulted in lower m values and weaker stress relaxation capacity. This implies that at $-18\text{ }^{\circ}\text{C}$, the asphalt had greater hardness and its performance was mainly determined by the internal network structure. The extensive intertwining in filamentous SBS morphology weakens the relaxation capability due to reduced topological freedom. At $-12\text{ }^{\circ}\text{C}$, where molecular motion within the asphalt is less restricted, greater intertwining leads to stronger network structure and enhanced stress relaxation capacity.

3.3. Impact of Pre-Cutting Process on the Chemical Composition and Aging Resistance Performance of SBS-Modified Asphalt

3.3.1. Impact of Pre-Cutting Process on the Chemical Composition of Modified Asphalt

For the purpose of comparing the impact of the pre-cutting process as a substitute for high-speed shearing on the chemical composition of SBS-modified asphalt, with conventionally processed SBS-modified asphalt as the control group, FTIR tests were conducted on SBS-modified asphalt prepared using the pre-cutting process, with particle sizes of 18-30 mesh and 30-100 mesh for the SBS, as described in Section 3.2. The results are shown in Figure 17.

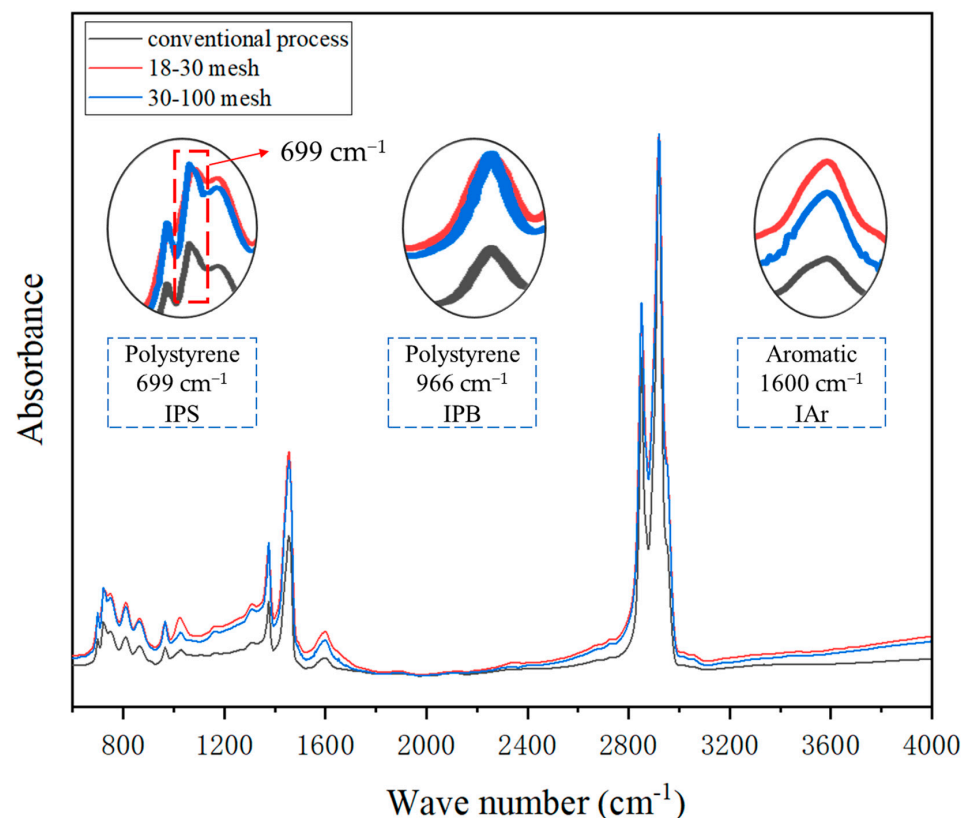


Figure 17. FTIR testing of SBS-modified asphalt prepared via pre-cutting process and conventional process.

It was observed that the characteristic peak areas of I_{PS} , I_{PB} , and I_{Ar} were larger in the SBS-modified asphalt prepared using the pre-cutting process. The peak areas of I_{PS} and I_{PB} were especially large, indicating that the pre-cutting process resulted in a higher dispersion concentration of SBS modifier within the asphalt, leading to better uniformity of dispersion. The larger peak area of I_{Ar} suggests that this might have been due to the longer processing time in the conventional method, resulting in a reduction in the aromatic content of the lighter components.

The characteristic peak parameters were calculated as shown in Figure 18. The feature parameters of the conventionally processed SBS-modified asphalt were consistently the smallest, consistent with the absorbance curve patterns. Upon comparing the progress of the two sets of SBS-modified asphalt samples prepared using the pre-cutting process, it was found that for the SBS pre-cut with a particle size of 30-100 mesh, both I_{PS} and I_{PB} were larger. This suggests that the smaller SBS particle size achieved through pre-cutting facilitated better dispersion within the asphalt, leading to higher concentrations of the detected characteristic peaks. However, for the SBS pre-cut with a particle size of 30-100 mesh, the I_{Ar} was smaller. This was due to the finer particle size of the SBS, which resulted in a larger contact area with the asphalt matrix. As a consequence, during the swelling process, a greater amount of light components was absorbed.

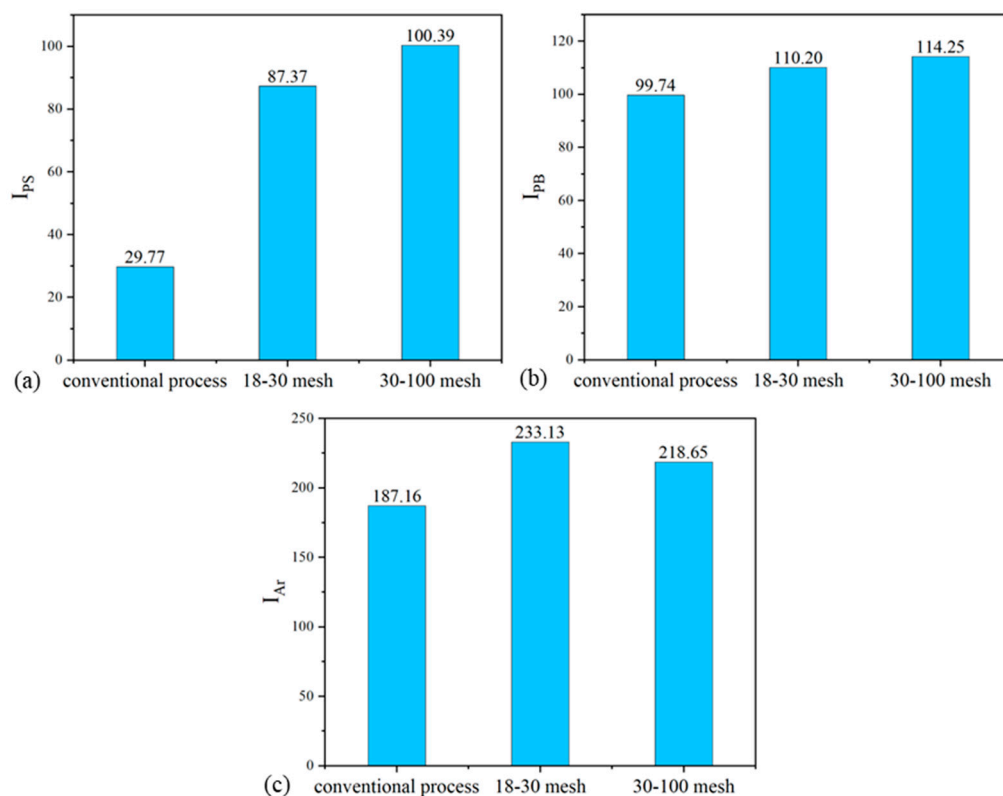


Figure 18. FTIR semi-quantitative analysis characteristics. (a) I_{PS} ; (b) I_{PB} ; (c) I_{Ar} .

3.3.2. Impact of Pre-Cutting as a Replacement for High-Speed Shearing Process on Anti-Aging Performance

The FTIR test results for the SBS-modified asphalt prepared with the pre-shredding process and the conventional process after PAV aging are shown in Figure 19. It can be observed that after aging, there was a prominent carbonyl peak at 1600 cm^{-1} in both SBS-modified asphalts, and the carbonyl peak area in the SBS-modified asphalt prepared via the conventional process was larger.

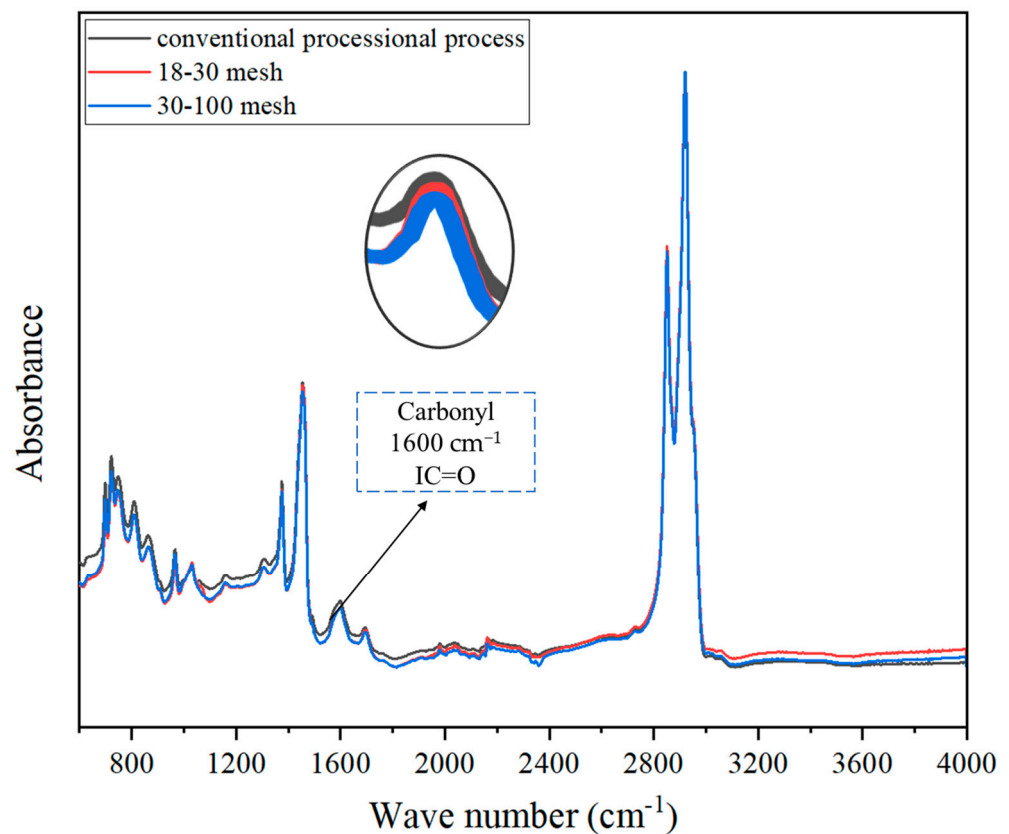


Figure 19. FTIR test chart after PAV aging.

The carbonyl index was calculated as shown in Figure 20. After PAV aging, the SBS-modified asphalt prepared via the conventional process had the highest carbonyl index, indicating the most severe aging. Compared to the conventional preparation process, when SBS was pre-shredded with a particle size of 18-30 mesh, the carbonyl index decreased by approximately 10%, and when the particle size was 30-100 mesh, the carbonyl index decreased by approximately 13%. This suggests that the new process of pre-shredding SBS resulted in improved aging resistance of the modified asphalt.

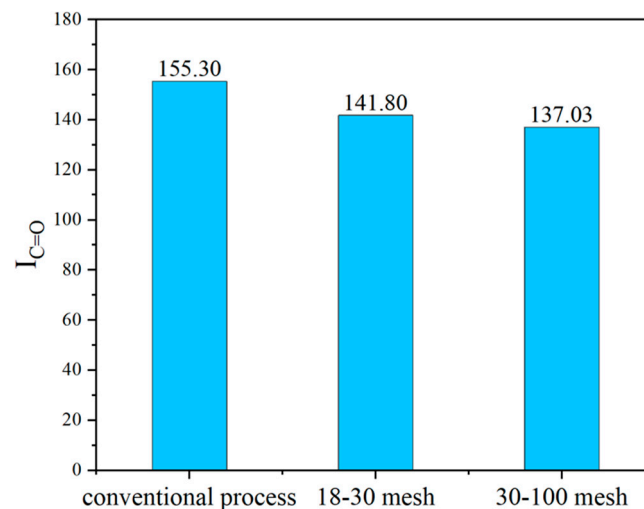


Figure 20. Carbonyl index after PAV aging.

For SBS with a particle size of 30-100 mesh, the improvement in aging resistance was more significant. This is because the finer SBS modifier was more evenly dispersed in

the base asphalt matrix, allowing for better heat and stress distribution. This reduced the occurrence of local hotspots and thermal stress, which helped to slow down the aging process.

4. Conclusions

- (1) The morphological changes of the SBS modifier in the preparation process through low-speed mixing can be summarized as follows: SBS edge networking, network filamentation, filament granulation, and granular atomization. The edge portions of the SBS particles absorb heat first, forming a network pore structure known as edge networking. As the network structure continues to absorb heat, it breaks apart to form a filamentary structure, known as network filamentation. Further heating leads to the fragmentation of the filamentary structure into multiple granular forms of SBS, known as filament granulation. This cycle of edge networking, network filamentation, and filament granulation is repeated multiple times until the SBS particles become extremely small, visually resembling a misty granular form, in a process known as granular atomization.
- (2) In the process of preparing modified asphalt through low-speed mixing with pre-cut SBS modifier, the mixing time should be controlled within 30 to 60 min to achieve uniform dispersion and excellent performance of the modified asphalt. If the mixing time is too short, the performance of the modified asphalt will be weaker than that of conventional-process asphalt. Pre-cut SBS-modified asphalt mixed for 30 to 60 min exhibits a filament–point combined morphology wherein the filamentous SBS enhances interlocking, resulting in a stronger network structure. This imparts excellent high-temperature rutting resistance, fatigue resistance, and low-temperature crack resistance. Mixing for 120 min results in a morphology with small granular particles resembling a mist. Interestingly, this morphology weakens the strength of the network structure and leads to a decrease in overall performance.
- (3) In the process of preparing modified asphalt through low-speed mixing with pre-cut SBS modifier, when the shredded SBS particle size is greater than 18 mesh, the resulting modified asphalt exhibits uniform dispersion and excellent performance. The SBS-modified asphalt prepared in this way features a filament–point combined morphology, leading to outstanding overall performance. When the particle size is in the range of 30 to 18 mesh, the modified asphalt benefits from larger filament widths and particle diameters, resulting in a stronger network structure and higher resistance to high-temperature rutting. On the other hand, at a particle size of 100 to 30 mesh, the modified asphalt possesses smaller filament widths and particle diameters, leading to better network structure extensibility and, consequently, improved performance in terms of mid-temperature fatigue resistance and low-temperature crack resistance.
- (4) Compared to the traditional method of preparing SBS-modified asphalt, the new process of using pre-shredded SBS instead of high-speed shearing reduces the overall preparation time by 1 to 3 h, resulting in lower energy consumption. Moreover, it improves aging resistance by 10% to 13%. Additionally, SBS-modified asphalt prepared using the new process demonstrates superior performance, thus reducing road wear and saving maintenance costs.
- (5) This research investigated the microstructure, three key indicators, rheological properties, and chemical composition of asphalt for which the pre-cutting process was used instead of high-speed shearing. It is anticipated that future research will comprehensively explore other aspects of performance, such as water damage resistance. Additionally, the asphalt mixture prepared using this process will be subjected to performance testing for road applications, including Hamburg wheel tracking test, semi-circular bend test (SCB), four-point bending fatigue test, and more. Finally, we hope to apply the pre-cutting process as a replacement for high-speed shearing to a wider range of modifiers, such as SEBS, EVA, and petroleum resins.

Author Contributions: Conceptualization, Y.W. and H.Y.; methodology, Y.C.; software, S.L.; validation, Y.W., H.Y. and S.Z.; formal analysis, Y.W.; investigation, Y.W. and C.Y.; resources, Y.W.; data curation, H.Y. and C.Y.; writing—original draft preparation, Y.W.; writing—review and editing, H.Y.; visualization, Y.C.; supervision, S.L.; project administration, S.Z.; funding acquisition, Y.W. All authors have read and agreed to the published version of the manuscript.

Funding: This research was funded by the National Key R&D program of China (2022YFB2602603); Hong Kong scholars program (XJ2022040); National Natural Science Foundation of China (52008353); Sichuan Youth Science and Technology Innovation Research Team (2021JDTD0023, 2022JDTD0015).

Institutional Review Board Statement: Not applicable.

Informed Consent Statement: Not applicable.

Data Availability Statement: Not applicable.

Conflicts of Interest: The authors declare no conflict of interest.

References

1. Chen, M.; Geng, J.; Xia, C.; He, L.; Liu, Z. A review of phase structure of SBS modified asphalt: Affecting factors, analytical methods, phase models and improvements. *Constr. Build. Mater.* **2021**, *294*, 123610. [\[CrossRef\]](#)
2. Khodaii, A.; Mehrara, A. Evaluation of permanent deformation of unmodified and SBS modified asphalt mixtures using dynamic creep test. *Constr. Build. Mater.* **2009**, *23*, 2586–2592. [\[CrossRef\]](#)
3. Zhang, D.; Zhang, H.; Shi, C. Investigation of aging performance of SBS modified asphalt with various aging methods. *Constr. Build. Mater.* **2017**, *145*, 445–451. [\[CrossRef\]](#)
4. Liang, M.; Xin, X.; Fan, W.; Luo, H.; Wang, X.; Xing, B. Investigation of the rheological properties and storage stability of CR/SBS modified asphalt. *Constr. Build. Mater.* **2015**, *74*, 235–240. [\[CrossRef\]](#)
5. Xu, S.; Fan, Y.; Feng, Z.; Ke, Y.; Zhang, C.; Huang, H. Comparison of quantitative determination for SBS content in SBS modified asphalt. *Constr. Build. Mater.* **2021**, *282*, 122733. [\[CrossRef\]](#)
6. Chen, J.S.; Liao, M.C.; Tsai, H.H. Evaluation and optimization of the engineering properties of polymer-modified asphalt. *Pract. Fail. Anal.* **2002**, *2*, 75–83. [\[CrossRef\]](#)
7. Sun, L.; Wang, Y.; Zhang, Y. Aging mechanism and effective recycling ratio of SBS modified asphalt. *Constr. Build. Mater.* **2014**, *70*, 26–35. [\[CrossRef\]](#)
8. Dong, F.; Zhao, W.; Zhang, Y.; Wei, J.; Fan, W.; Yu, Y.; Wang, Z. Influence of SBS and asphalt on SBS dispersion and the performance of modified asphalt. *Constr. Build. Mater.* **2014**, *62*, 1–7. [\[CrossRef\]](#)
9. Wen, G.; Zhang, Y.; Zhang, Y.; Sun, K.; Fan, Y. Improved properties of SBS-modified asphalt with dynamic vulcanization. *Polym. Eng. Sci.* **2002**, *42*, 1070–1081. [\[CrossRef\]](#)
10. Liu, L.; Liu, Z.H.; Li, S. The Preparation Technology and Performance Study of SBS and Rubber Powder Composite Modified Asphalt. *Appl. Mech. Mater.* **2013**, *361–363*, 1617–1620. [\[CrossRef\]](#)
11. Cao, Z.; Chen, M.; Yu, J.; Han, X. Preparation and characterization of active rejuvenated SBS modified bitumen for the sustainable development of high-grade asphalt pavement. *J. Clean. Prod.* **2020**, *273*, 123012. [\[CrossRef\]](#)
12. Zhou, Z.; Chen, G. Preparation, Performance, and modification mechanism of high viscosity modified asphalt. *Constr. Build. Mater.* **2021**, *310*, 125007. [\[CrossRef\]](#)
13. Wang, Y.; Yi, H.; Liang, P.; Chai, C.; Yan, C.; Zhou, S. Investigation on Preparation Method of SBS-Modified Asphalt Based on MSCR, LAS, and Fluorescence Microscopy. *Appl. Sci.* **2022**, *12*, 7304. [\[CrossRef\]](#)
14. Kaya, D.; Topal, A.; McNally, T. Relationship between processing parameters and aging with the rheological behaviour of SBS modified bitumen. *Constr. Build. Mater.* **2019**, *221*, 345–350. [\[CrossRef\]](#)
15. Ozdemir, D.K.; Topal, A.; McNally, T. Relationship between microstructure and phase morphology of SBS modified bitumen with processing parameters studied using atomic force microscopy. *Constr. Build. Mater.* **2021**, *268*, 121061. [\[CrossRef\]](#)
16. Zhang, C.; Wang, H.; You, Z.; Gao, J.; Irfan, M. Performance test on Styrene-Butadiene-Styrene (SBS) modified asphalt based on the different evaluation methods. *Appl. Sci.* **2019**, *9*, 467. [\[CrossRef\]](#)
17. Ye, F.; Yin, W.; Lu, H.; Dong, Y. Property improvement of Nano-Montmorillonite/SBS modified asphalt binder by naphthenic oil. *Constr. Build. Mater.* **2020**, *243*, 118200. [\[CrossRef\]](#)
18. Dong, F.; Fan, W.; Yang, G.; Wei, J.; Luo, H.; Wu, M.; Zhang, Y. Dispersion of SBS and its Influence on the Performance of SBS Modified Asphalt. *J. Test. Eval.* **2014**, *42*, 1073–1080. [\[CrossRef\]](#)
19. Wang, T.; Yi, T.; Yuzhen, Z. The compatibility of SBS-modified asphalt. *Pet. Sci. Technol.* **2010**, *28*, 764–772. [\[CrossRef\]](#)
20. Larsen, D.O.; Alessandrini, J.L.; Bosch, A.; Cortizo, M.S. Micro-structural and rheological characteristics of SBS-asphalt blends during their manufacturing. *Constr. Build. Mater.* **2009**, *23*, 2769–2774. [\[CrossRef\]](#)
21. Kaya, D.; Topal, A.; Gupta, J.; McNally, T. Aging effects on the composition and thermal properties of styrene-butadiene-styrene (SBS) modified bitumen. *Constr. Build. Mater.* **2020**, *235*, 117450. [\[CrossRef\]](#)

22. Wu, S.; He, R.; Chen, H.; Li, W.; Li, G. Rheological properties of SBS/CRP composite modified asphalt under different aging treatments. *Materials* **2020**, *13*, 4921. [[CrossRef](#)]
23. Yu, C.; Hu, K.; Yang, Q.; Chen, Y. Multi-scale observation of oxidative aging on the enhancement of high-temperature property of SBS-modified asphalt. *Constr. Build. Mater.* **2021**, *313*, 125478. [[CrossRef](#)]
24. Lin, P.; Huang, W.; Li, Y.; Tang, N.; Xiao, F. Investigation of influence factors on low temperature properties of SBS modified asphalt. *Constr. Build. Mater.* **2017**, *154*, 609–622. [[CrossRef](#)]
25. Wu, S.P.; Pang, L.; Mo, L.T.; Chen, Y.C.; Zhu, G.J. Influence of aging on the evolution of structure, morphology and rheology of base and SBS modified bitumen. *Constr. Build. Mater.* **2009**, *23*, 1005–1010. [[CrossRef](#)]
26. Zhang, H.L.; Su, M.M.; Zhao, S.F.; Zhang, Y.P.; Zhang, Z.P. High and low temperature properties of nano-particles/polymer modified asphalt. *Constr. Build. Mater.* **2016**, *114*, 323–332. [[CrossRef](#)]
27. D'Angelo, J.; Dongré, R. Practical use of multiple stress creep and recovery test: Characterization of styrene-butadiene-styrene dispersion and other additives in polymer-modified asphalt binders. *Transp. Res. Rec.* **2009**, *2126*, 73–82. [[CrossRef](#)]
28. Wang, Y.; Polaczyk, P.; He, J.; Lu, H.; Xiao, R.; Huang, B. Dispersion, compatibility, and rheological properties of graphene-modified asphalt binders. *Constr. Build. Mater.* **2022**, *350*, 128886. [[CrossRef](#)]
29. Geng, L.; Liu, Y.; Xu, Q.; Han, F.; Yu, X.; Qin, T. Development of bio-based stabilizers and their effects on the performance of SBS-modified asphalt. *Constr. Build. Mater.* **2021**, *271*, 121889. [[CrossRef](#)]
30. Liu, J.; Hao, P.; Jiang, W.; Sun, B. Rheological properties of SBS modified asphalt incorporated polyvinylpyrrolidone stabilized graphene nanoplatelets. *Constr. Build. Mater.* **2021**, *298*, 123850. [[CrossRef](#)]
31. Yao, X.; Li, C.; Xu, T. Multi-scale studies on interfacial system compatibility between asphalt and SBS modifier using molecular dynamics simulations and experimental methods. *Constr. Build. Mater.* **2022**, *346*, 128502. [[CrossRef](#)]
32. Kang, Y.; Song, M.; Pu, L.; Liu, T. Rheological behaviors of epoxy asphalt binder in comparison of base asphalt binder and SBS modified asphalt binder. *Constr. Build. Mater.* **2015**, *76*, 343–350. [[CrossRef](#)]
33. Yan, K.; You, L.; Wang, D. High-temperature performance of polymer-modified asphalt mixes: Preliminary evaluation of the usefulness of standard technical index in polymer-modified asphalt. *Polymers* **2019**, *11*, 1404. [[CrossRef](#)] [[PubMed](#)]
34. Fu, H.; Xie, L.; Dou, D.; Li, L.; Yu, M.; Yao, S. Storage stability and compatibility of asphalt binder modified by SBS graft copolymer. *Constr. Build. Mater.* **2007**, *21*, 1528–1533. [[CrossRef](#)]
35. Wang, J.; Qin, Y.; Huang, S.; Xu, J. Laboratory Evaluation of Aging Behaviour of SBS Modified Asphalt. *Adv. Mater. Sci. Eng.* **2017**, *2017*, 3154634. [[CrossRef](#)]
36. Zhang, W.; Ma, T.; Xu, G.; Huang, X.; Ling, M.; Chen, X.; Xue, J. Fatigue Resistance Evaluation of Modified Asphalt Using a Multiple Stress Creep and Recovery (MSCR) Test. *Appl. Sci.* **2018**, *8*, 417. [[CrossRef](#)]
37. Huang, W.; Tang, N. Characterizing SBS modified asphalt with sulfur using multiple stress creep recovery test—ScienceDirect. *Constr. Build. Mater.* **2015**, *93*, 514–521. [[CrossRef](#)]
38. Ma, T.; Huang, X.; Zhao, Y.; Yuan, H. Aging behaviour and mechanism of SBS-modified asphalt. *J. Test. Eval.* **2012**, *40*, 1186–1191. [[CrossRef](#)]
39. Liu, X.; Cao, F.; Xiao, F.; Amirkhanian, S. BBR and DSR testing of aging properties of polymer and polyphosphoric acid-modified asphalt binders. *J. Mater. Civ. Eng.* **2018**, *30*, 04018249. [[CrossRef](#)]
40. Campos-Lopez, E.; McIntyre, D.; Fetters, L.J. Thermodynamic and structural properties of polystyrene-polybutadiene-polystyrene block copolymers. *Macromolecules* **1973**, *6*, 415–423. [[CrossRef](#)]

Disclaimer/Publisher's Note: The statements, opinions and data contained in all publications are solely those of the individual author(s) and contributor(s) and not of MDPI and/or the editor(s). MDPI and/or the editor(s) disclaim responsibility for any injury to people or property resulting from any ideas, methods, instructions or products referred to in the content.